Biophysical Chemistry 196 (2015) 33–39

Contents lists available at ScienceDirect

Biophysical Chemistry

journal homepage: http://www.elsevier.com/locate/biophyschem

Lipid composition is an important determinant of antimicrobial activity of alpha-melanocyte stimulating hormone

Tahsina Shireen [a,1], Arnab Basu [b,1], Munna Sarkar [b], Kasturi Mukhopadhyay [a,*]

[a] School of Environmental Sciences, Jawaharlal Nehru University, New Delhi 110067, India
[b] Chemical Sciences Division, Saha Institute of Nuclear Physics 1/AF, Bidhannagar, Kolkata 700064, India

HIGHLIGHTS

- α-MSH preferentially interacts with anionic vesicles.
- Interaction with vesicles does not induce any secondary structure in α-MSH.
- α-MSH causes permeabilization and lysis of vesicles having negatively charged lipid.
- Both permeabilization and lysis by α-MSH are dependent on peptide concentration.

GRAPHICAL ABSTRACT

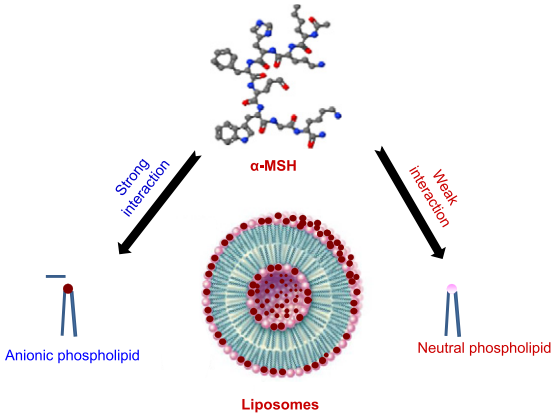

ARTICLE INFO

Article history:
Received 1 August 2014
Received in revised form 12 September 2014
Accepted 12 September 2014
Available online 22 September 2014

Keywords:
Antimicrobial peptide
Peptide-membrane interaction
Membrane permeabilization
Trp-fluorescence
Dynamic light scattering
Circular dichroism spectroscopy

ABSTRACT

We have reported strong antimicrobial activity of cationic neuropeptide α-MSH against *Staphylococcus aureus*. Clinical *S. aureus* isolates non-susceptible to the peptide had higher amount of cationic phospholipid. To elucidate the molecular basis of lipid selectivity and antimicrobial activity of α-MSH, studies were carried out on SUVs having different combinations of neutral DMPC and anionic lipids DMPG to mimic mammalian and bacterial membrane. The peptide interacted with the DMPG containing vesicles only, as evident from the changes in Trp fluorescence. CD spectroscopy revealed that despite interaction, the peptide retained its native random coil structure. The perturbation of the vesicles caused by peptide interaction is strongly dependent on peptide concentration as seen both by DLS and Tb^{3+}/DPA based fluorescence leakage assay. Our data clearly demonstrate the preference of α-MSH to interact with anionic DMPG containing vesicles leading to significant permeabilization which is the molecular basis behind the selectivity of α-MSH for bacterial systems.

1. Introduction

Antimicrobial peptides (AMPs) have been hailed as a potential solution to the dearth of novel antibiotic development in the past 50 years. AMPs are produced by almost all organisms and are relatively small (6–100 amino acids) molecules of variable length, sequence and

Abbreviations: α-MSH, alpha-melanocyte stimulating hormone; DMPC, 1,2-dimyristoyl-sn-glycero 3 phosphocholine; DMPG, 1,2-dimyristoyl-sn-glycero-3-glycerol; DLS, dynamic light scattering; CD, circular dichroism; SUV, small unilamellar vesicles; Tb^{3+}/DPA, Terbium/dipicolinic acid.

* Corresponding author. Tel.: +91 26704307; fax: +91 9871955700.
E-mail address: kasturim@mail.jnu.ac.in (K. Mukhopadhyay).

[1] Both the authors have equal contribution.

http://dx.doi.org/10.1016/j.bpc.2014.09.002
0301-4622/

structure with activity against a wide range of microorganisms. Despite these variations, the key features that render them to exhibit microbicidal activity are i) their cationicity and ii) their binding and adoption of secondary structural conformation in membrane environments [1]. These characteristics allow them to attach to and insert into the bacterial membrane rather than host membranes. Mostly all AMPs are understood to target the bacterial plasma membrane directly rather than through specific protein receptors [2]. Therefore the phospholipid composition, in particular the net charge of the membranes plays a vital role in determining the antimicrobial activity of the AMPs [3]. A number of studies have recently demonstrated that the introduction of positive charges on bacterial surface lowers the electrostatic interaction between AMPs and bacteria, thus increasing bacterial resistance [3]. Several liposomal models have been proposed to explain the bacterial membrane damage by AMPs and it has been shown that the threshold concentration of AMPs is an essential factor to achieve their antimicrobial activity. Below a threshold concentration, there is little activity despite binding; but when the concentration exceeds the threshold, the activity is at its maximum [4]. For example, in a very recent model membrane study it was shown that at lower peptide-lipid molar ratio of 1:250–1:350, the activity of human α-defensin HNP-1 is prevalently localized on membrane surface, which can bring to a thinning and destabilization of phospholipid bilayer. On increasing peptide concentration to 1:20, penetration and pore formation is the more suitable mechanism of action [5]. Despite numerous experimental and simulation studies on the mechanism of action of various AMPs, the underlying mechanism, like how AMPs perturb the membrane, remains enigmatic [6]. There are studies where certain membrane-active peptides like cecropins, magainins and mellitins have been demonstrated to permeabilize model membrane systems, leading to leakage of fluorescent dyes from unilamellar vesicles, or induce transport across lipid bilayers [2].

Alpha-melanocyte stimulating hormone (α-MSH, Ac-Ser-Tyr-Ser-Met-Glu-His-Phe-Arg-Trp-Gly-Lys-Pro-Val-NH_2), is an endogenous linear tridecapeptide known for its role in regulating skin pigmentation in vertebrates [7]. Beside this primary role, it also has many other biological functions like anti-inflammatory, neuroprotective, antipyretic and anti-apoptotic effects through binding to melanocortin G protein-coupled receptors (MCR) [8–11]. Recently we have demonstrated the antimicrobial activity of this cationic neuropeptide against the opportunistic pathogen *Staphylococcus aureus* (*S. aureus*) in vitro and in vivo as well. Furthermore we demonstrated that bacterial membrane damage is the primary mechanism of antibacterial activity of the peptide [12,13]. Very recently, our group also showed that α-MSH was least toxic to the mammalian cell line and it did not cause hemolysis of RBCs [14]. In another recent study by our group, it was found that clinical isolates of *S. aureus* that were non-susceptible to α-MSH had comparatively more amount of cationic phospholipid, lysylphosphatidylglycerol (LPG) and less amount of anionic phospholipid, phosphatidylglycerol (PG) in their membrane [15]. Taken together it looks like α-MSH preferentially interacts with negatively charged membrane and like any other cationic AMP, charge seems to be an important factor in the antimicrobial action of α-MSH.

It is postulated that permeabilization of the membrane by AMPs depends on peptide structure and phospholipid matrix. A number of studies have been reported on the behavior of α-MSH and its analogues in model membranes made of differentially charged phospholipids [16–19]. Most of them elucidated the structure-activity of the melanotropins and indicated that the structure and stability of α-MSH in negatively charged membrane were substantially different from those of the peptide in solution; being stabilized in a specific conformation that could be important to elicit its biological activity [18,20–22]. Previous reports have clearly indicated that α-MSH was able to interact and penetrate membranes. A two-step process was described: an initial electrostatic interaction between the positively charged peptide with negatively charged lipids of the membrane by which it reaches an appropriate local concentration and then the penetration of the peptide in the hydrophobic core of the bilayer [20,21,23,24]. The secondary structure of α-MSH in membrane-mimetic solvent 2,2,2-trifluoroethanol (TFE) is reported to be random coil [25]. However, the activity of α-MSH in different combinations of anionic and neutral lipids has not been explored. Taking these observations into consideration, in the present study we focused to understand the role of lipid composition in antibacterial activity of α-MSH. Here, we have studied in detail the interaction of α-MSH in simple membrane mimetic like Small Unilamellar Vesicles (SUVs) that are easy to prepare with reproducible average diameter and diameter size distribution. SUV's were formed by the phospholipid, dimyristoylphosphatidylcholine (DMPC) with zwitterionic headgroups i.e. with no net charge and dimyristoylphosphatidylglycerol (DMPG) with anionic headgroups. DMPC was chosen to mimic surface membrane of mammalian cells because the lipid is stable to oxidation and readily hydrates in water forming lamellar phases at physiological pH and temperatures. DMPG was chosen since phosphatidylglycerol is absent in eukaryotic plasma membranes but is ubiquitous and abundant in bacterial membranes. We have prepared SUVs composed of different ratios of DMPC and DMPG. This was done to modulate the negative charge on the vesicle surface. Carefully designed controls using dynamic light scattering (DLS) were used to look at the stability of the vesicles under the experimental conditions studied. Stability was assessed by the invariance of the average diameter and the size distribution with increasing standing time of the sample. DLS was also used to observe changes in the average vesicular diameter and size distribution, if any, in the presence of varying concentration of the peptide. We have measured the changes in the tryptophan (Trp) fluorescence of α-MSH in the various combinations of DMPC and DMPG SUVs to see if there is any difference in the interaction of the peptide with these vesicles. Circular dichroism (CD) spectroscopy was used in the far-ultraviolet region to monitor the changes in the secondary structures of the peptide in different membrane environments. Finally, we have performed the leakage assay with terbium/dipicolinic acid (Tb^{3+}/DPA) in order to examine the effect of increasing concentrations of α-MSH on the rate of permeabilization of differentially charged phospholipids. This assay monitors the rate and extent of the leakage of the inner aqueous content of the vesicles into the bulk aqueous phase, which in turn measures the perturbing effect of the peptide on vesicles. The detail of the leakage assay is provided in the next section.

2. Materials and methods

DMPC [1,2-dimyristoyl-*sn*-glycero-3-phosphocholine] and DMPG [1,2-dimyristoyl-*sn*-glycero-3-phosphor-*rac*-(1-glycerol) sodium salt], TritonX-100 (ultrapure), dipicolinic acid (DPA), terbium (Tb^{3+}) chloride, sephadex G-50, and alpha-melanocyte stimulating hormone (α-MSH) were purchased from Sigma-Aldrich (St. Louis, MO). The concentration of α-MSH was determined spectrophotometrically (Shimadzu UV-2450 spectrophotometer). 2-[tris(hydroxymethyl)-methylamine]-1-ethanesulfonic acid (TES buffer) and sodium ethylene diamine tetra-acetate (EDTA sodium salt) were purchased from SRL (India), and all were used without further purification.

2.1. Preparation of SUVs

Small unilamellar vesicles of DMPC, DMPG and combinations of the lipids up to the ratio of 50:50 DMPC:DMPG were prepared by the method of sonication as described elsewhere [26]. Briefly, phospholipids were weighed and dissolved in 2:1 (v/v) chloroform:methanol solution and the solvent was evaporated by purging argon to prepare the lipid film. It was then dried overnight in a vacuum desiccator at −20 °C. The dried film was hydrated and swelled in 10 mM TES, pH 7.4 for CD spectra and fluorescence measurements. For DLS study, SUVs were prepared by dissolving lipid films in double filtered 10 mM MOPS (3-N-morpholino propanesulfonic acid) buffer. For leakage assay, dried film was hydrated and swelled in 10 mM TES and 60 mM NaCl at pH 7.4 for $TbCl_3$ (8 mM)

containing vesicles and 10 mM TES at pH 7.4 for dipicolinic acid (DPA) (80 mM) vesicles. The mixture was vortexed to disperse lipids. The dispersion was then sonicated for about 10 min using Dr. Hielscher (Germany) probe sonicator (200 W). The samples were then allowed to stand for 40 min to be hydrated completely. The sonicated samples were centrifuged at 12,000 rpm for 15 min to remove titanium particles and aggregated lipids. To ensure that the experiments were carried on SUVs that are in their sol phase, the temperature of the sample was kept at 37 °C for all subsequent measurements which also happens to be the physiologically relevant temperature.

2.2. Fluorescence measurements

All fluorescence measurements were done with a Hitachi 4500 spectrofluorimeter (Japan), which was operated in L-format. The excitation wavelength was 280 nm and emission was recorded at a range of 300–400 nm. Slits of 2.5 nm were used in both the excitation and emission side throughout the experiment [27]. A peptide-lipid ratio (P/L) of 0.02 was used in all the 3 combinations of DMPC:DMPG, namely 100% DMPC, 70:30 DMPC:DMPG and 50:50 DMPC:DMPG.

2.3. Dynamic light scattering

Hydrodynamic number weighted size and size distribution of different SUVs were determined by DLS using the instrument ZetaSizer NanoS of Malvern Instruments; Worcestershire, UK. The instrument operates at 90° scattering angle and 173° detection geometry. All experiments were carried out at 37 °C and other parameters like material, dispersant were set according to the nature of the experiment. In case of SUVs, polystyrene latex and 10 mM Tris were taken as material and dispersant respectively. The particle scattering intensity is proportional to the square of the molecular weight. The intensity distribution can be somewhat misleading since scattering intensity from only a small amount of aggregates or larger particles can dominate the distribution. Results of experiments were therefore interpreted in terms of number percentage with respect to the diameter of the molecules. Here number signifies the number of different sized particles that exist in solution and the percentage indicates relative abundance of each size involved in scattering. This was done to better observe the relative changes in the size and distribution of the small vesicles used here, that are not obscured by the presence of a small number of larger vesicles or aggregates.

2.4. Circular dichroism spectroscopy

CD spectra of α-MSH in the absence and presence of different combinations of SUVs were measured on a Jasco J-720 Spectropolarimeter at 37 °C, using a 1 mm path length quartz cell to minimize the absorbance due to buffer components. A P/L ratio of 0.02 was used in all the combinations of DMPC:DMPG. The following scan parameters were used: 1 nm band width, 2 s response time, 0.1 nm step resolution and 50 nm min^{-1} scan speed. Each spectrum was an average of six scans, recorded from 190–250 nm and the molar ellipticity [θ] was given in $deg \cdot cm^2 \cdot dmol^{-1}$. The baselines of blank or vesicular suspension without peptide were subtracted from each sample.

2.5. Leakage assay

Leakage assays are used to measure the extent of permeabilization/perturbation of vesicular structure by different agents such as antimicrobial peptides (AMPs) and drugs. Here the leakage assay was done by co-encapsulating $TbCl_3$ and DPA in vesicles as described in our previous work [26]. Both $TbCl_3$ and DPA are weakly fluorescent molecules but co-encapsulation in vesicles results in the formation of strongly fluorescent chelated Tb^{3+}/DPA complex. Tb^{3+} (8 mM) and DPA (80 mM) co-encapsulated vesicles were prepared in 10 mM TES buffer at pH 7.4. They were chromatographed on a Sephadex G-50 column equilibrated with 10 mM TES buffer, pH 7.4, 100 mM NaCl, containing 1 mM EDTA, to eliminate unbound $TbCl_3$ in the external buffer. When leakage of inner aqueous contents (where co-encapsulated $TbCl_3$ and DPA reside as fluorescent Tb^{3+}/DPA complex) occurs in the presence of different peptide concentrations, a drop in fluorescence intensity is observed. This is because EDTA, present in the external buffer is a stronger chelator of DPA than Tb^{3+} which dissociates the strongly fluorescent Tb^{3+}/DPA complex to form Tb–EDTA complex. This leads to a decrease in the fluorescence intensity. The decrease in fluorescence intensity was measured at 490 nm with an excitation wavelength at 275 nm using a HORIBA Jobin Yvon Spex Fluoromax-3 spectrofluorimeter. Three different P/L ratios were used, 0.02, 0.04 and 0.06. The temperature was kept constant at 37 °C. To express the fluorescence intensity decay in terms of percentage leakage, 0% leakage was characterized by the fluorescence intensity of vesicles containing co-encapsulated Tb^{3+}/DPA with added peptide recorded at time t = 0 and 100% leakage was characterized by the fluorescence intensity of the co-encapsulated Tb^{3+}/DPA vesicles lysed with 0.1% (w/v) Triton X-100, which completely disrupts the vesicles. Measurements were made relative to the fluorescence intensity of detergent released vesicles. Thus the percent leakage was calculated as:

$$\%\ \textbf{leakage} = \frac{\left(F^{d,t=0}{}_{CO} - F^{d,det}{}_{CO}\right) - \left(F^{d,t}{}_{CO} - F^{d,det}{}_{CO}\right)}{F^{d,t=0}{}_{CO} - F^{d,det}{}_{CO}} \times 100$$

$F^{d,t=0}{}_{CO}$ Fluorescence intensity of Tb^{3+}/DPA co-encapsulated vesicles in the presence of peptide at the time t = 0 (first data in the kinetics measurement).

$F^{d,t}{}_{CO}$ Fluorescence intensity of Tb^{3+}/DPA co-encapsulated vesicles in presence of peptide at time 't'.

$F^{d,det}{}_{CO}$ Fluorescence intensity of Tb^{3+}/DPA co-encapsulated vesicles after lysing with 0.1% (w/v)TritonX-100.

The time courses of the leakage assay obtained by plotting % leakage vs time were fit to single exponential [f = a{1 − exp(−kt)}] curves using non-linear least square fitting program of Origin 8.0. The extent of leakage at infinite time is given by the pre-exponential factor 'a' and 'k' denotes the rate constant. Parameter uncertainties are expressed as the standard deviations (SD) of data for at least three different measurements.

3. Results

3.1. Integrity of the vesicles followed by dynamic light scattering (DLS) studies

In order to characterize the prepared vesicles and check their integrity with time, DLS was used. As mentioned before, DLS spectra are represented as number % instead of intensity %, so that the relative changes in the size and size distribution of these small vesicles is not obscured by the presence of a few large vesicles or aggregates. This is because scattering intensity is proportional to the square of the molecular weight and intensity from a small amount of large particles can dominate the distribution. Fig. 1A shows the plot of the relative percentage in numbers vs the diameter for 100% DMPC vesicles with different standing times. With increasing time, the average diameter of the vesicles as well as the distribution width, depicted by the width of the peak, shows no significant changes indicating that the vesicles maintain their integrity and do not undergo either spontaneous lysis or aggregation to form vesicles with smaller or larger average diameter. The same is true for vesicles formed with 50:50 DMPC:DMPG (Fig. 1B). Fig. 1C shows the DLS plots of 100% DMPG vesicles with increasing time. The average diameter shifts with increasing time to progressively smaller

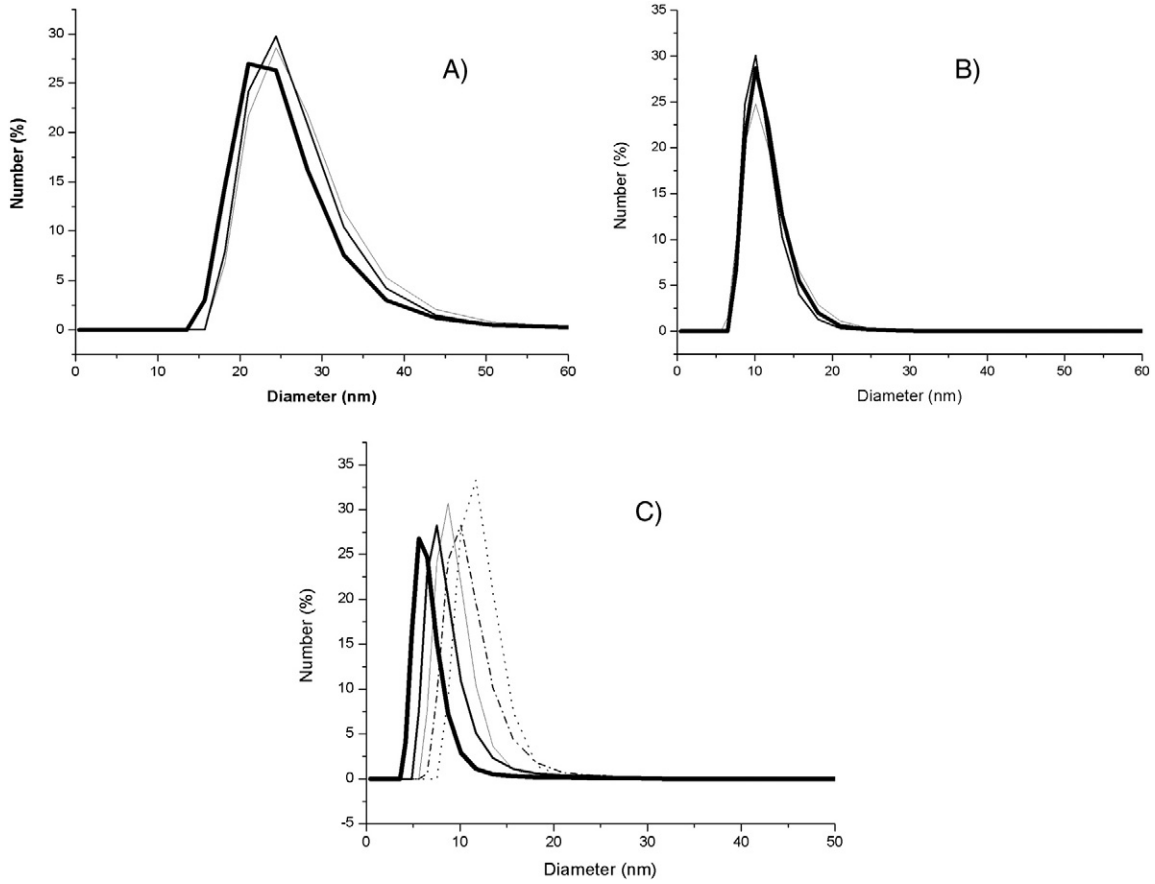

Fig. 1. Dynamic light scattering profile expressed in number weighted size and size distribution (Number %) vs diameter (nm) for SUVs having [A] 100% DMPC with DLS recorded after a standing time of 5 min (-), 10 min (-) and 15 min (-); [B] 50:50 DMPC:DMPG mixed vesicles with DLS recorded after 5 min (-), 10 min (-), 15 min (-)] and [C] 100% DMPG with DLS recorded after 2 min (····), 5 min (·–·–·–·), 8 min (-), 11 min (-), and 14 min (-).

values. This demonstrates that under the experimental conditions studied, vesicles formed from pure DMPG cannot maintain their integrity and undergo spontaneous lysis forming smaller sized vesicles. Hence, for subsequent experiments, mixed vesicles having DMPG more than 50% were not used.

3.2. Interaction of α-MSH with vesicles followed by fluorescence spectroscopy and DLS

Traditionally changes in Trp fluorescence which includes peak shift and fluorescence quantum yields have long been known to be sensitive to the polarity of its local environment and have been used as a probe to monitor variations in the local structure and dynamics of a protein or peptide. Presently, changes in the Trp peak and quantum yield have been attributed to microscopic changes in the protein environment. It is now accepted that ^1L_a state is responsible for Trp fluorescence. Upon excitation to this state the electron density shifts from the pyrole ring to the benzene ring thereby making it sensitive to the solvent dielectric constant [28]. In general, a larger dielectric solvent will result in large red shift while the opposite is true for less polar solvents. The reason behind the changes in the Trp quantum yield that makes the intensity sensitive to the local environment is the presence of a close charge transfer (CT) state near the ^1L_a state. This CT band is produced by the electron transfer from the indole ring to the nearest backbone amide in the protein/peptide. Fluorescence quenching occurs when the CT state is stabilized enough to move below the ^1L_a state in the presence of strong local electric fields as in aqueous solvents and hydrogen bonding solvents [29]. In our case, α-MSH has one Trp residue. Fig. 2 displays the Trp emission spectra of α-MSH in aqueous buffer and in the presence of different mixed vesicles having increasing concentration of DMPG. A blue shift and a variation in quantum yield are expected when the peptide interacts with the vesicles that alter the Trp microenvironments [30]. The emission maximum of α-MSH in buffer is 350 nm. In pure DMPC vesicles i.e. 100% DMPC, the emission maximum is also seen at the same wavelength (Fig. 2) with similar intensity which indicates that there is no interaction of the peptide with pure DMPC vesicles. For all other DMPG containing SUVs, a clear blue shift of Trp emission was observed (Fig. 2) with a maximum shift to 340 nm in case of 50:50 DMPC:DMPG. There was also a substantial increase in fluorescence

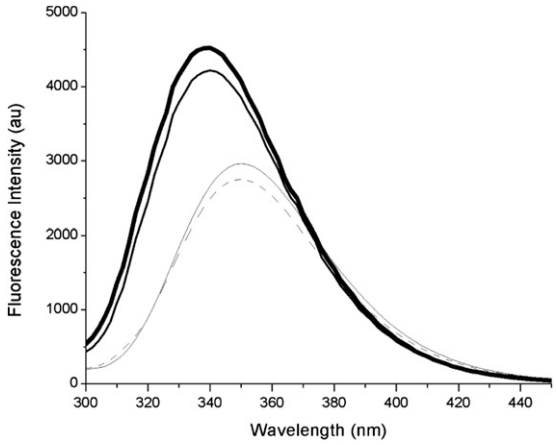

Fig. 2. Fluorescence spectra of α-MSH peptide (30 μM, P/L = 0.02) in the presence of DMPC and DMPG containing mixed vesicles with varying composition as indicated in the figure, α-MSH in buffer (———); in DMPC:DMPG 100:0 (-); DMPC:DMPG 70:30 (-); and DMPC:DMPG 50:50 (-).

intensity for the mixed vesicles. This shows that α-MSH binds with these vesicles.

Fig. 3 shows the plot of the relative % in numbers vs the diameter for 50:50 DMPC:DMPG vesicles on interacting with increasing concentration of α-MSH. At relatively small concentration of 30 μM (P/L = 0.02) of α-MSH, it interacts with the vesicles to form peptide–vesicle complex which results in larger average hydrodynamic diameter compared to the control, having the same mixed vesicles but in the absence of the peptide. At higher concentration of 60 μM (P/L = 0.04), α-MSH starts perturbing the vesicles, permeabilizing and disrupting the vesicular structure. This obliterates the interaction of the peptide with the majority of the vesicles, thereby resulting in gradual restoration of average diameter to that of the control mixed vesicles in the absence of the peptide. However, in this case there is also a residual contribution in the range of the diameter of the peptide–vesicle complex as indicated by the broader width of the DLS spectra compared to the control, indicating the presence of mixed population consisting of peptide–SUV complexes and free SUVs. In the presence of the highest concentration (90 μM, P/L = 0.06), the average diameter is restored to that of the mixed vesicles in the absence of the peptide which indicates that almost all the vesicles lose their interaction with peptide molecules. The slightly larger width of the DLS spectra than the control, points to the presence of a very small fraction of vesicles superficially bound to the peptide. The reduction in relative % in numbers compared to the control may be an indication of destruction of some vesicles due to lysis producing such small aggregates that are beyond the detection limit of the instrument.

3.3. Changes in secondary structure of α-MSH from CD spectroscopy

Some membrane active peptides change their secondary structure upon interaction with the lipid bilayer [31]. To investigate the effect of the membrane-mimicking environments on the conformational changes of α-MSH (30 μM), the CD spectra of the peptide in buffer and in SUVs of different combinations of DMPC and DMPG were examined as shown in Fig. 4. In aqueous buffer, CD spectrum of α-MSH is predominantly in the random coil form. Despite binding to the different mixed SUVs, there is no significant change in the secondary structure of α-MSH which remained predominantly in random coil conformation. Below 210 nm the spectra are too noisy and smoothing could not remove all the noise. Therefore, no significance should be associated with changes in the spectral profile below 210 nm.

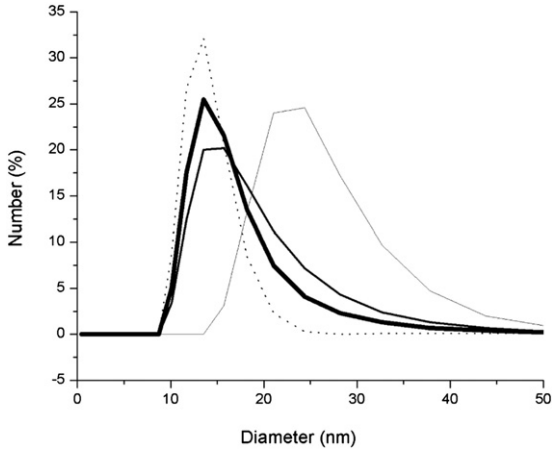

Fig. 3. Dynamic light scattering profile expressed in number weighted size and size distribution (number %) vs diameter (nm) of 50:50 DMPC:DMPG vesicles in absence (·····) and in the presence of 30 μM α-MSH (P/L = 0.02) (-); 60 μM α-MSH (P/L = 0.04) (-) and 90 μM of α-MSH (P/L = 0.06) (-). Samples were incubated with the peptide for 5 min in each case before DLS measurements.

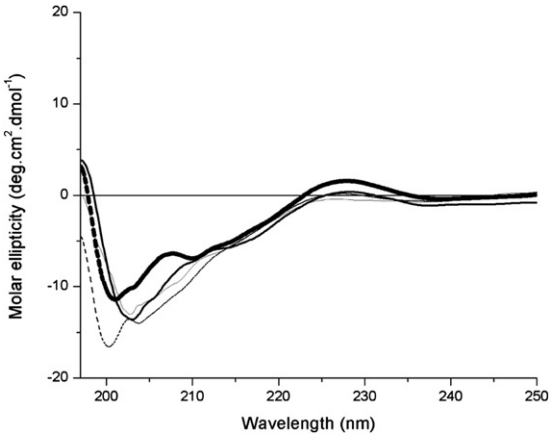

Fig. 4. CD spectra of (30 μM, P/L = 0.02) α-MSH (-) in the presence of different mixed vesicles as indicated in the figure [(100:0) DMPC:DMPG (——), (70:30) DMPC:DMPG (-) and (50:50) DMPC:DMPG (———)]. All spectra were smoothed with Savitzky–Golay smoothing function.

3.4. Leakage assay indicates membrane perturbation by α-MSH

In our previous reports we have established that α-MSH causes membrane permeabilization and release of cellular contents in *S. aureus* [12,13]. Here, the extent of inner aqueous content leakage both spontaneous and under the influence of the peptide within the same time frame was studied by standard terbium Tb^{3+}/dipicolinic acid (DPA) assay in liposomal model. From the plots of % leakage as a function of time (as described in Materials and methods section), the rate and extent of leakage which is a measure of the perturbing ability of the peptide, was calculated for mixed lipid systems with varying concentration of peptide. The values are listed in Table 1. Fig. 5A and B shows representative plots of % leakage vs time for DMPC:DMPG 50:50 vesicles in the presence and absence of 30 μM (P/L = 0.02) α-MSH. For pure DMPG vesicles, instability sets in even in the absence of the peptide as seen from our DLS data (Fig. 1C) and hence was not considered for the leakage studies. Stable vesicles that do not undergo spontaneous lysis have only been considered. In DMPC:DMPG 70:30, leakage of contents was observed upon addition of 30 and 60 μM of the peptide beyond which the vesicles were lysed. With the addition of higher concentration of peptide (90 μM) lysis was indicated by a very fast drop in the fluorescence intensity due to the sudden exposure of Tb^{3+}/DPA complex to the external aqueous phase where it was disrupted by the presence of EDTA. For 30 μM peptide concentration, the rate was not affected compared to that of the control but there is an increase in the extent. At 60 μM peptide concentration even though the rates decreased but the extent remained same. Similarly for DMPC:DMPG 50:50, leakage of contents could be measured for 30 and 60 μM concentrations of the peptide without the vesicles being completely destabilized, with the rate and extent remaining unaffected (within the experimental error limit) on the addition of 30 μM peptide compared to the control. In

Table 1
Leakage rate 'k' (sec^{-1}) and extent 'a' (%) in different vesicles induced by various concentrations of α-MSH.

DMPC:DMPG ratio	α-MSH (μM) [peptide/lipid]	Rate (k ± SD) (sec^{-1})[a]	Extent (a ± SD) (%)[a]
DMPC70: DMPG30	0	$(7.61 \pm 0.15) \times 10^{-4}$	(38.43 ± 0.26)
	30 [0.02]	$(7.99 \pm 0.15) \times 10^{-4}$	(40.55 ± 0.27)
	60 [0.04]	$(2.19 \pm 0.17) \times 10^{-4}$	(40.23 ± 2.07)
DMPC50: DMPG50	0	$(7.28 \pm 0.39) \times 10^{-4}$	(6.7 ± 0.11)
	30 [0.02]	$(5.81 \pm 1.31) \times 10^{-4}$	(6.45 ± 0.06)
	60 [0.04]	$(36.3 \pm 2.40) \times 10^{-4}$	(14.23 ± 0.59)

[a] Each set of experiment has been repeated for 3 times to get the standard deviation.

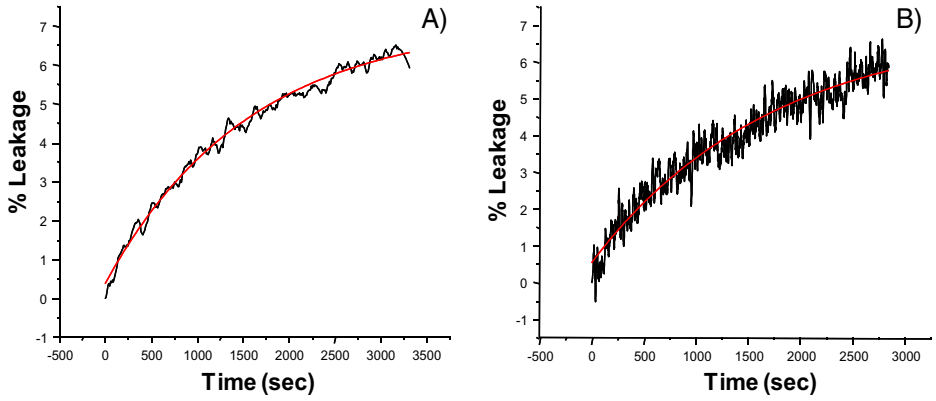

Fig. 5. Representative plot of % leakage vs time (s) of mixed vesicles of DMPC:DMPG (50:50) in (A) **the** absence and (B) in the presence of 30 μM (P/L = 0.02) α-MSH. The leakage profile is fitted to a single exponential rate equation, f = a [1-exp(-kt)], where 'k' measured the rate of leakage and 'a' measured the extent of leakage i.e. the % leakage at infinite time. The fitted curve is superimposed in red.

case of 60 μM α-MSH, there is a large increase in leakage rate as well as an increase in extent. For 90 μM peptide, the leakage rates were too high beyond the measurement ability of our instrument. Since there was no binding of the peptide to pure DMPC SUVs as seen from our fluorescence data, leakage was not studied for these vesicles.

4. Discussion

It is well known that the presence of positive charge and hydrophobic residues of peptides and lipid composition of membranes are the determinants of the activity of AMPs [1,3,32–34]. In earlier studies, α-MSH has been shown to cause membrane perturbation and leakage of entrapped fluorescent dye in the major human pathogen *S. aureus* [12,13]. Since α-MSH has one positive net charge it is suggested that its antimicrobial activity is guided by electrostatic interactions with the bacterial membranes. To further elucidate whether this cationic neuropeptide specifically acts on the negatively charged membranes, we applied model membranes composed of different mixtures of neutral (DMPC) and anionic (DMPG) phospholipids. Whereas, PC headgroups are prevalent in the cytoplasmic membranes of humans, PG headgroups dominates *S. aureus*.

Many interesting observations emanated from our investigation. From the Trp fluorescence emission spectra analysis, a clear blue shift and an increase in intensity was observed in all DMPG comprising mixed vesicles compared to the spectra of the peptide in buffer, while there was no shift in the wavelength maxima or intensity increase in SUV containing only DMPC. It very clearly points out that α-MSH interacts with DMPG containing vesicles i.e., negatively charged membranes penetrating deep enough to alter the Trp environment. Likewise increase in fluorescence intensity and a blue shift was observed in the case of the cationic HNP-1 upon interacting with negatively charged vesicles [5]. Pep-1, a cell-penetrating peptide showed a similar kind of blue shift of Trp fluorescence when bound to negatively charged vesicles and very small shift in the presence of zwitterionic vesicles [35]. Therefore we infer that α-MSH possibly interacts with the vesicles from its C-terminal end and penetrates into the hydrocarbon region of negatively charged lipids rather than neutral SUVs. Another way of measuring membrane penetration by a peptide is to incorporate fluorescence probe tagged lipids into the bilayer. These probes are chosen for their ability to accept energy transfer from the Trp residue of the interacting peptide. Forster Resonance Energy Transfer (FRET) from Trp to the probe measures the penetration of the peptide into the bilayer [36]. Our DLS data on the interaction of increasing concentration of the peptide with 50:50 DMPC:DMPG vesicles, yields very interesting results. At lower concentration, the peptide partially penetrates the vesicles forming peptide–vesicle complex with effective hydrodynamic diameter higher than the vesicles without the peptide. For the peptide, penetrating from the C-terminal end [13] that also requires at least the involvement of the Trp residue, the expected increase in diameter is not more that 2–5 nm [37]. The large increase in diameter of 10–12 nm on forming peptide–vesicular complex could be due to peptide oligomerization on the vesicle surface and/or increased number of peptide association per liposome. This is consistent with other AMPs at similar P/L ratio. Such oligomerization and/or increased peptide association per liposome would perturb vesicles and permeabilize the liposomes as shown by previous researchers [5]. The existence of a threshold concentration of the peptide is an important requirement to cause membrane penetration with subsequent permeabilization which has been aptly demonstrated in case of Human Neutrophil Peptide 1, with liposomes [5]. This is what we see even in our case. Higher α-MSH concentration, promotes peptide oligomerization and/or increased peptide association per liposome leading to membrane permeabilization. Further increase in the concentration of the peptide leads to the lysis of the vesicles which manifests the loss of interaction with peptides. This results in a mixed population of peptide–vesicles complex and peptide free vesicles as seen in the case of 60 μM α-MSH at P/L ratio of 0.04. At even higher concentration of 90 μM, P/L = 0.06, most of the vesicles lose their interaction with the peptide due to lysis.

From CD spectroscopy analysis, the secondary structure of α-MSH was found to be predominantly random coil, both in buffer and all SUVs of different ratios of DMPC and DMPG. This indicates that change in the environment from polar to apolar does not alter the conformation of the peptide. Similarly in a study by Steffen et al., where they examined the behavior of different dermicidin-derived peptides, found that neither the cationic nor the anionic dermicidin peptides changed their conformation of a random coil in an aqueous buffer to alpha helix when incubated with unilamellar liposomes of DOPC and DOPG–DOPC [38]. In another study, defensins were shown to interact strongly with negatively charged membranes causing fusion and lysis. Trp fluorescence spectroscopy also revealed shifts in the wavelength maximum in the presence of negatively charged liposomes and no change in a neutral environment. However conformational studies revealed that defensins did not change its native structure of β-sheet in the presence of either neutral or negatively charged liposomes [39]. Our study which is in concordance with these findings indicates that the overall structure of α-MSH is maintained upon interaction with lipid bilayers, while binding and permeabilizing the membranes composed of anionic lipids.

Finally, from the leakage assay, it was observed that in the presence of the peptide additional permeabilization of the vesicles took place followed by release of contents in the SUVs consisting of DMPG. The extent of perturbation of the vesicles by α-MSH increased with increasing concentration of the peptide as reflected by either the increase in rates or the extent of leakage. Beyond a particular threshold concentration which varied with the composition of the vesicles, there was a complete lysis. In the case of 50:50 DMPC:DMPG, which shows maximum interaction with

the peptide as seen from our fluorescence studies, the situation is very interesting. Our DLS data as well as leakage assay results indicate that at lower concentration of the peptide there is interaction with the vesicles without significant additional permeabilization. Increasing concentration of α-MSH results in enhanced leakage and at 90 μM (P/L = 0.06), the leakage rates become too fast which was beyond our measurement limit. Therefore, we can undoubtedly conclude that α-MSH specifically interacts with anionic membrane environments and its activity is more pronounced in SUVs having mixtures of DMPC and DMPG. The perturbing ability of the peptide is both dependent on its concentration as well as the vesicular composition where negative charge variation is an important determining parameter for membrane interaction and perturbation by α-MSH.

5. Conclusion

Overall, this work gives additional insights into the mode of antimicrobial action of cationic neuropeptide α-MSH. From this study we could find that α-MSH particularly embeds in the anionic membrane environment and causes membrane perturbation and the mode of perturbation is both peptide concentration and membrane composition dependent. The insertion of peptides into the SUVs does not change the overall conformation of the peptide, which remains in the random coil state as seen from our CD data. Thus, our study has strengthened the importance of the electrostatic interaction as a key factor involved in the α-MSH antibacterial activity and at the same time illustrates that threshold peptide concentration and the presence of negatively charged lipid membrane could be crucial for the biological activity of cationic α-MSH.

Acknowledgments

This study was supported by grants to K.M. from the Indian Council of Medical Research (5/3/3/24/2010-ECD-I) and the Department of Biotechnology (BT/PR9582/Med/29/34/2007), India. T.S. acknowledges fellowship from the University Grants Commission, India.

References

[1] R.E.W. Hancock, D.S. Chapple, Peptide antibiotics, Antimicrob. Agents Chemother. 43 (1999) 1317–1323.
[2] L. Zhang, A. Rozek, R.E.W. Hancock, Interaction of cationic antimicrobial peptides with model membranes, J. Biol. Chem. 276 (2001) 35714–35722.
[3] M.R. Yeamen, N.Y. Yount, Mechanisms of antimicrobial peptide action and resistance, Pharmacol. Rev. 55 (2003) 27–54.
[4] M.-T. Lee, W.-C. Hung, F.-Y. Chen, H.W. Huang, Mechanism and kinetics of pore formation in membranes by water soluble amphipathic peptides, PNAS 105 (2008) 5087–5092.
[5] A. Bonucci, E. Balducci, S. Pistolesi, R. Pogni, The defensin-lipid interaction: insights on the binding states of the human antimicrobial peptide HNP-1 to model bacterial membranes, Biochim. Biophys. Acta 1828 (2013) 758–764.
[6] J. Li, S. Liu, R. Lakshminarayan, Y. Bai, K. Pervushin, C. Verma, R.W. Beuerman, Molecular simulations suggest how a branched antimicrobial peptide perturbs a bacterial membrane and enhances permeability, Biochim. Biophys. Acta 1828 (2013) 1112–1121.
[7] J.M. Lipton, A. Catania, Anti-inflammatory influence of the neuro immunomodulator alpha-MSH, Immunol. Today 18 (1997) 140–145.
[8] A. Catania, J.M. Lipton, Alpha-Melanocyte stimulating hormone in the modulation of host reactions, Endocr. Rev. (1993) 564–576.
[9] A. Catania, The melanocortin system in leukocyte biology, J. Leukoc. Biol. 81 (2007) 383–392.
[10] A. Catania, Neuroprotective actions of melanocortins: a therapeutic opportunity, Trends Neurosci. 31 (2008) 353–360.
[11] A. Catania, C. Lonati, A. Sordi, A. Carlin, S. Gatti, The melanocortin system in control of inflammation, Sci. World J. 10 (2010) 1840–1853.
[12] Madhuri, T. Shireen, S.K. Venugopal, D. Ghosh, R. Gadepalli, B. Dhawan, K. Mukhopadhyay, In vitro antimicrobial activity of alpha-melanocyte stimulating hormone against major human pathogen *Staphylococcus aureus*, Peptides 30 (2009) 1627–1635.
[13] M. Singh, K. Mukhopadhyay, C-terminal amino acids of alpha-melanocyte stimulating hormone are requisite for its antibacterial activity against *Staphylococcus aureus*, Antimicrob. Agents Chemother. 55 (2011) 1920–1929.
[14] M. Singh, R. Gadepalli, B. Dhawan, K. Mukhopadhyay, Combination of alpha melanocyte stimulating hormone with conventional antibiotics against methicillin resistant *Staphylococcus aureus*, PLoS One 8 (2013) e73815.
[15] T. Shireen, M. Singh, B. Dhawan, K. Mukhopadhyay, Characterization of cell membrane parameters of clinical isolates of *Staphylococcus aureus* with varied susceptibility to alpha-melanocyte stimulating hormone, Peptides 37 (2012) 334–339.
[16] V.J. Hruby, S.D. Sharma, K. Toth, J.Y. Jaw, F. al-Obeidi, T.K. Sawyer, et al., Design, synthesis, and conformation of superpotent and prolonged acting melanotropins, Ann. N. Y. Acad. Sci. 680 (1993) 51–63.
[17] M.E. Hadley, S.D. Sharma, V.J. Hruby, N. Levine, R.T. Dorr, Melanotropic peptides for therapeutic and cosmetic tanning of the skin, Ann. N. Y. Acad. Sci. 680 (1993) 424–439.
[18] D.L. de Souza, B. Frisch, G. Duportail, F. Schuber, Membrane-active properties of α-MSH analogs: aggregation and fusion of liposomes triggered by surface-conjugated peptides, Biochim. Biophys. Acta 1558 (2002) 222–237.
[19] R.M. Fernandez, A.S. Ito, H.B. Schiöth, M.T. Lamy, Structural study of melanocortin peptides by fluorescence spectroscopy: identification of β-(2-napthyl)-D-alanine as a fluorescent probe, Biochim. Biophys. Acta 1623 (2003) 13–20.
[20] M.H. Biaggi, K.A. Riske, M.T. Lamy-Freund, Melanotropic peptides-lipid bilayer interaction. Comparison of the hormone alpha-MSH to a biologically more potent analog, Biophys. Chem. 67 (1997) 139–149.
[21] A.S. Ito, A.M. Castrucci, V.J. Hruby, M.E. Hadley, D.T. Krajcarsk, A.G. Szabo, Structure-activity correlations of melanotropin peptides in model lipids by tryptophan fluorescence studies, Biochemistry 32 (1993) 12264–12272.
[22] L.M. Contreras, R.F.M. de Almeida, J. Villalaín, A. Fedorov, M. Prieto, Interaction of α-melanocyte stimulating hormone with binary phospholipid membranes: structural changes and relevance of phase behaviour, Biophys. J. 80 (2001) 2273–2283.
[23] M.H. Biaggi, S. Schreier, A.M. Castrucci, M.T. Lamy-Freund, Interaction of melanotropic peptides with lipid membranes, Ann. N. Y. Acad. Sci. 680 (1993) 459–461.
[24] M.H. Biaggi, T.J. Pinheiro, A. Watts, M.T. Lamy-Freund, Spin label and 2H-NMR studies on the interaction of melanotropic peptides with lipid bilayers, Eur. Biophys. J. 24 (1996) 251–259.
[25] K. Mukhopadhyay, S. Basak, Conformation induction in melanotropic peptides by trifluoroethanol: fluorescence and circular dichroism study, Biophys. Chem. 74 (1998) 175–186.
[26] S. Mondal, M. Sarkar, Non-steroidal anti-inflammatory drug induced membrane fusion: concentration and temperature effects, J. Phys. Chem. 113 (2009) 16323–16331.
[27] H. Chakraborty, S. Mondal, M. Sarkar, Membrane fusion: a new function of non steroidal anti-inflammatory drugs, Biophys. Chem. 137 (2008) 28–34.
[28] J.T. Vivian, P.R. Callis, Mechanisms of tryptophan fluorescence shifts in proteins, Biophys. J. 80 (2001) 2093–2109.
[29] P.L. Muiño, P.R. Callis, Solvent effects on the fluorescence quenching of tryptophan by amides via electron transfer. Experimental and computational studies, J. Phys. Chem. B 113 (2009) (2009) 2572–2577.
[30] B. Christianes, S. Symoens, S. Vanderheyden, Y. Englborghs, A. Joliot, A. Prochiants, J. Vandekerckhove, M. Rosseneu, B. Vanloo, Tryptophan fluorescence study of the interaction of penetrating peptides with model membranes, Eur. J. Biochem. 269 (2002) 2918–2926.
[31] M. Magzoub, L.E. Eriksson, A. Graslund, Conformational states of the cell-penetrating peptide penetratin when interacting with phospholipids vesicles: effects of surface charge and peptide concentration, Biochim. Biophys. Acta 1563 (2002) 53–63.
[32] M. Zasloff, Antimicrobial peptides of multicellular organisms, Nature 24 (1987) 389–395.
[33] K.A. Brodgen, Antimicrobial peptides: pore formers or metabolic inhibitors in bacteria? Nat. Rev. Microbiol. 3 (2005) 238–250.
[34] K.V.R. Reddy, R.D. Yedery, C. Aranha, Antimicrobial peptides: premises and promises, Int. J. Antimicrob. Agents 24 (2004) 536–547.
[35] W.L. Zhu, Hahm, S.Y. Shin, Cell selectivity and mechanism of action of short antimicrobial peptides designed from the cell-penetrating peptide Pep-1, J. Pept. Sci. 15 (2009) 569–575.
[36] P.F. Almeida, A. Pokorny, Binding and permeabilization of model membranes by amphipathic peptides, Methods Mol. Biol. 618 (2010) 155–169.
[37] N.C. Fitzkee, G.D. Rose, Reassessing random coil statistics in unfolded proteins, PNAS (2004) 12497–12502.
[38] H. Steffen, S. Rieg, I. Weidermann, H. Kalbacher, et al., Naturally processed dermicidin-derived peptides do not permeabilize bacterial membranes and kill microorganisms irrespective of their charge, Antimicrob. Agents Chemother. 50 (2006) 2608–2620.
[39] G. Fujii, M.E. Selsted, D. Eisenberg, Defensins promote fusion and lysis of negatively charged membranes, Protein Sci. 2 (1993) 1301–1312.